Cavity Quantum Electrodynamics Effects with Nitrogen Vacancy Center Spins Coupled to Room Temperature Microwave Resonators

Yuan Zhang,* Qilong Wu, Shi-Lei Su, Qing Lou, and Chongxin Shan†
Henan Key Laboratory of Diamond Optoelectronic Materials and Devices, Key Laboratory of Material Physics, Ministry of Education, School of Physics and Microelectronics, Zhengzhou University, Daxue Road 75, Zhengzhou 450052, China

Klaus Mølmer‡
Aarhus Institute of Advanced Studies, Aarhus University, Høegh-Guldbergs Gade 6B, DK-8000 Aarhus C, Denmark; Center for Complex Quantum Systems, Department of Physics and Astronomy, Aarhus University, Ny Munkegade 120, DK-8000 Aarhus C, Denmark

(Received 1 November 2021; accepted 17 May 2022; published 24 June 2022)

Cavity quantum electrodynamics (CQED) effects, such as Rabi splitting, Rabi oscillations, and superradiance, have been demonstrated with nitrogen vacancy (NV) center spins in diamond coupled to microwave resonators at cryogenic temperature. In this Letter, we explore the possibility to realize strong collective coupling and CQED effects with ensembles of NV spins at room temperature. Our calculations show that thermal excitation of the individual NV spins leads to population of collective Dicke states with low symmetry and a reduced collective coupling to the microwave resonators. Optical pumping can be applied to counteract the thermal excitation of the NV centers and to prepare the spin ensemble in Dicke states with high symmetry. The resulting strong coupling with high-quality resonators enables the study of intriguing CQED effects across the weak-to-strong coupling regime, and may have applications in quantum sensing and quantum information processing.

DOI: 10.1103/PhysRevLett.128.253601

Introduction.—Cavity quantum electrodynamics (CQED) studies the interaction between quantum emitters and cavity photon modes, and is used for studies of quantum mechanics foundations [1], quantum information processing [2], and quantum metrology [3]. CQED effects, such as Rabi splitting [4–6], Rabi oscillations [7], and superradiance [8], have been realized with negatively charged nitrogen vacancy (NV^-) center spins in diamond inside microwave resonators at cryogenic temperature. Although the NV^- spins have a spin-1 degree of freedom, normally only two of the spin states, say those with projections $m = 0$ and $m = +1$, are coupled resonantly to the resonator, and thus the spins can be treated effectively as two-level systems. As illustrated in Fig. 1(a), at low temperature the spin ensemble can be highly polarized, and can thus couple strongly and collectively with lumped-element microwave resonators with high Q factor.

The low temperature restricts the application of the CQED effects in quantum sensing and quantum information processing, and it would be desirable if the collective coupling could be achieved at room temperature. In this Letter, we show theoretically that the CQED effects can be achieved at room temperature if the NV^- spin ensemble is coupled to a high-quality dielectric resonator and continuously cooled by optical pumping, see Fig. 1(b). In our analysis, we use the Dicke state picture to analyze the

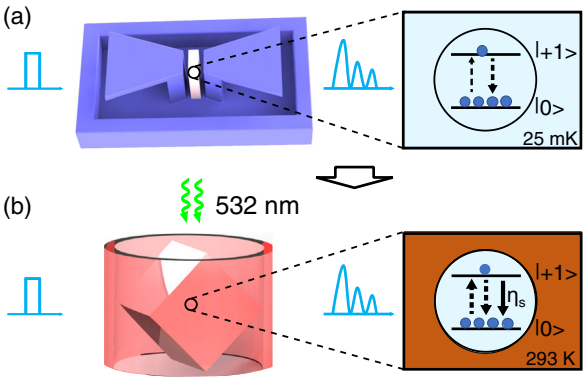

FIG. 1. CQED systems with a NV center spin ensemble. Panel (a) shows a 3D lumped element resonator at 25 mK (left), as used in [8], where the spin-ensemble is in equilibrium with the cooled environment (right). Panel (b) shows a sapphire dielectric resonator operating at room temperature, as used in [9], and a diamond illuminated by 532 nm laser (left), which counteracts the heating of the spins by the hot environment (right), leading to a higher population in the lower 0 spin state. The dashed and solid arrows represent the spin-lattice relaxation and the optical spin-cooling, modeled effectively by a decay rate η_s from the upper to lower spin state. Incident square microwave field pulses and outgoing modulated signal pulses are indicated by the blue curves.

influence of the hot environment on the spin ensemble, and the ability of the optical spin cooling to actively control the collective coupling with the resonator. We demonstrate that this control permits the exploration of intriguing CQED effects across different regimes of weak and strong coupling in the same physical system. Note that the collective coupling may have been present in the recent room-temperature experiments on continuous-wave maser [9], dispersive readout of NV^- spins [10,11], and CQED effects with the lowest triplet spin states of pentacene molecules [12].

Nitrogen vacancy center spin ensemble.—Nitrogen vacancy centers are formed by replacing two adjacent carbon atoms with a nitrogen atom and a vacancy in the diamond lattice. Negatively charged NV^- centers have a triplet electronic ground state with three spin states of projection $m = +1, 0, -1$ along the nitrogen-vacancy axis. The ± 1 spin states have higher energy than the 0 state, and can be split and shifted by a static magnetic field. In this way, the transition between one of the shifted states and the 0 state can be tuned into resonance with a microwave resonator. Furthermore, the magnetic field can be aligned along one of four possible nitrogen-vacancy orientations to ensure that only the associated $0, +1$ or $0, -1$ spin states couple resonantly with the microwave resonator. In this case, these spin states can be viewed as the eigenstates of a pseudo $1/2$-spin, and N NV^- centers can be viewed as an ensemble of N pseudo spins.

Dicke representation of spin collective states.—The collective coupling of the $1/2$-spin ensemble with the resonator is conventionally described by the so-called Dicke states $|J, M\rangle$ [13]. The half-integer or integer number $J \leq J_0 = N/2$ refers to the eigenvalues $J(J+1)$ of the collective spin operator $\vec{J}^2$, and the number M within the range $-J \leq M \leq J$ describes the degree of spin excitation. For each J, the Dicke states of different M form a vertical ladder, and the horizontally shifted ladders with different J form a triangular domain [Fig. 2(a)].

The uniform coupling to the microwave resonator and the individual (but identical) incoherent excitation and decay processes can be consistently and effectively treated as transitions among the Dicke states [16–18]. In Fig. 2(a), we show how the spin-lattice relaxation, which deexcites and excites the individual spin with the rates γ_s^- and γ_s^+, causes quantum jumps that change M by ± 1 and J by $0, \pm 1$ (blue and red arrows), while the optical spin-cooling adds a term η_s to the rate γ_s^- of downward jumps (blue arrows). A pure single-spin dephasing rate χ_s is incorporated to effectively describe the phase noise and inhomogeneous broadening of the transition frequencies, and leads to quantum jumps to states with unchanged M and different J (black arrows), while the coherent collective coupling with the resonator (with g_s as the single-spin coupling strength) causes transitions between states of different M and same J (orange arrow). The actual rates also depend on

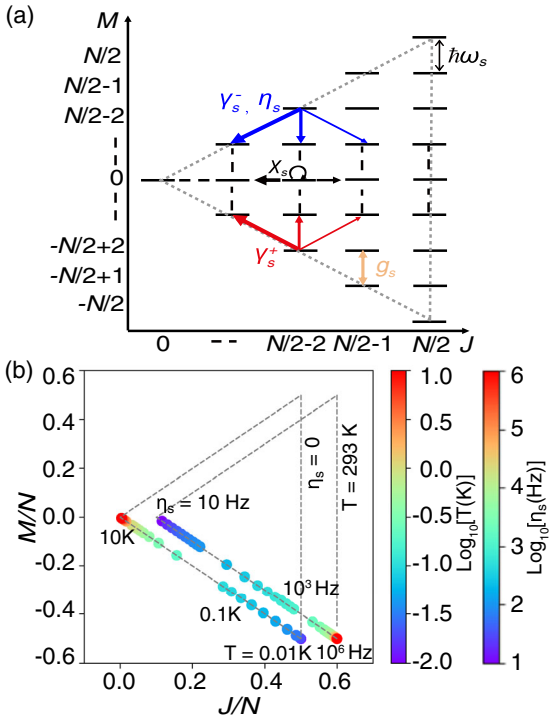

FIG. 2. Panel (a) shows the Dicke states of the NV^- spin ensemble with transition frequency ω_s, and the quantum jumps associated with downward spin-lattice relaxation γ_s^- and optical spin cooling η_s (blue arrows), upward spin-lattice relaxation γ_s^+ (red arrows), spin dephasing χ_s (horizontal black arrows), and collective coupling to the resonator (orange double arrow). The transition rates have further dependencies on the Dicke state quantum numbers J and M, and the thickness of the arrows represents their relative variation. Panel (b) shows the steady-state Dicke state population for different temperatures T in the absence of the optical spin cooling $\eta_s = 0$ (left), and for different η_s at room temperature $T = 293$ K (right, shifted horizontally for clarity) for parameters compatible with the Rabi-splitting experiment at cryogenic temperature [7], see Sec. S4 of [14].

the J and M quantum numbers, and for combinatorial reasons the jump probability is larger toward the Dicke states with reduced J (and decreased coupling) as reflected by the thickness of the arrows, see Appendix A in [16] for precise expressions.

In the presence of the spin-lattice relaxation and the optical spin cooling, each spin is in a mixed steady state with the upper state population, $p = \gamma_s^+/(\eta_s + \gamma_s^+ + \gamma_s^-)$. This is equivalent to a distribution on the Dicke states [19], with average values M, J of the Dicke states quantum numbers $M = J_0(2p-1)$, and $J(J+1) = (2p-1)^2 J_0(J_0+1) + 6p(p-1)J_0$. For many spins, the relative fluctuations of these quantities are small, and we may thus depict the location of the Dicke states populated by the spin ensemble as a point in the diagram as in Fig. 2(b).

Without the optical spin cooling $\eta_s = 0$, the spin ensemble occupies Dicke states with smaller J for temperature above $T > 10$ K, and occupies the states with larger J

(lower-right corner) only for $T < 0.01$ K, see the dots along the lower boundary of the left triangle in Fig. 2(b). As the collective spin-resonator coupling scales with $\sqrt{J}$, the spin-ensemble has to be held at very low temperature to ensure the strong collective coupling. In contrast, with sufficient optical spin cooling η_s (values up to 1 MHz should be achievable [20]) to compensate the spin-lattice relaxation, the spin ensemble can be prepared in Dicke states with larger J and strong collective coupling to the microwave resonator, cf., the dots along the rightmost triangle in Fig. 2(b). In Sec. S1 of [14], we provide extra results to estimate quantitatively the cooling of the spin-ensemble and the coupled microwave resonator mode [21]. In the calculations presented below, we shall employ a mean-field approach as in [12,20,22,23], and use the Dicke state representation for visualization and interpretation of the results. Note that the spin-ensemble cooling at room temperature discussed here is fundamentally different from the rapid dephasing-induced and Purcell-enhanced spin cooling via a cavity mode coupled to a cold environment, as proposed in Ref. [24].

Quantum master equation.—To assess the CQED effects with the NV$^-$ spin ensemble-microwave resonator system at room temperature, we employ a two-level description of the spins and solve the quantum master equation for the density operator $\hat{\rho}$,

$$\begin{aligned}\frac{\partial}{\partial t}\hat{\rho} = &-\frac{i}{\hbar}[\hat{H}_c + \hat{H}_d + \hat{H}_s + \hat{H}_{s-c}, \hat{\rho}] \\ &- \kappa_c[(1+n_c^{th})\mathcal{D}[\hat{a}]\hat{\rho} + n_c^{th}\mathcal{D}[\hat{a}^\dagger]\hat{\rho}] \\ &- \gamma_s^- \sum_j \mathcal{D}[\hat{\sigma}_j^{12}]\hat{\rho} - \gamma_s^+ \sum_j \mathcal{D}[\hat{\sigma}_j^{21}]\hat{\rho} \\ &- \eta_s \sum_j \mathcal{D}[\hat{\sigma}_j^{12}]\hat{\rho} - 2\chi_s \sum_j \mathcal{D}[\hat{\sigma}_j^{22}]\hat{\rho}, \end{aligned} \tag{1}$$

where $\hat{H}_c = \hbar\omega_c \hat{a}^\dagger \hat{a}$ describes the microwave resonator with frequency ω_c, photon creation $\hat{a}^\dagger$ and annihilation operator $\hat{a}$, $\hat{H}_d = \hbar\Omega\sqrt{\kappa_1}\hat{a}e^{i\omega_d t} + \text{H.c.}$ describes the driving of the resonator by a microwave probe field with amplitude Ω, frequency ω_d and the coupling coefficient $\sqrt{\kappa_1}$ (κ_1 is the resonator loss rate due to the same coupling). The spin Hamiltonian $\hat{H}_s = \hbar\omega_s \sum_{j=1}^N \hat{\sigma}_j^{22}$ involves the transition frequency ω_s and the projection operator $\hat{\sigma}_j^{22}$ on the upper level of the jth spin. The spin-resonator interaction Hamiltonian $\hat{H}_{s-c} = \hbar g_s(\hat{a}^\dagger \sum_j \hat{\sigma}_j^{12} + \sum_j \hat{\sigma}_j^{21}\hat{a})$ depends on the lowering $\hat{\sigma}_j^{12}$ and raising operators $\hat{\sigma}_j^{21}$ of the spin transitions.

The second line of Eq. (1) describes the thermal emission and excitation of the resonator with a rate κ_c and a thermal equilibrium photon number $n_c^{th} = [e^{\hbar\omega_c/k_BT} - 1]^{-1}$ at temperature T (with Boltzmann constant k_B). Here, the Lindblad superoperator for any operator $\hat{o}$ is defined as $\mathcal{D}[\hat{o}]\hat{\rho} = \frac{1}{2}(\hat{o}^\dagger\hat{o}\,\hat{\rho} + \hat{\rho}\hat{o}^\dagger\hat{o}) - \hat{o}\,\hat{\rho}\,\hat{o}^\dagger$. The third line describes the spin-lattice relaxation with rates γ_s^+, γ_s^-, which are dominated by the single phonon process at extremely low temperature [25], and the second-order Raman scattering and Orbach-type process at high temperature [26]. In the fourth line, the rates η_s, χ_s describe the optical pumping-induced spin cooling involving higher excited states [21], and the total dephasing due to the interaction with the spin bath and the inhomogeneous broadening of spin transition frequencies. We have verified that the results are qualitatively preserved, when the optical spin cooling and the spin dephasing are described more precisely with a multi-level [27] and multiensemble [28] interaction model.

To solve Eq. (1), we apply a mean-field approach [22,23] (also known as the cluster-expansion method [29]) and apply the equation $(\partial/\partial t)\langle\hat{o}\rangle = \text{tr}\{[(\partial/\partial t)\hat{\rho}]\hat{o}\}$ for the mean value $\langle\hat{o}\rangle = \text{tr}\{\hat{\rho}\,\hat{o}\}$ of any operator $\hat{o}$, and truncate the resulting equation hierarchy by approximating the mean values of products of many operators with those of fewer operators. To simulate system with trillions of spins, we assume same parameters ω_s, γ_s^+, γ_s^-, η_s, χ_s for all the NV$^-$ spins and, hence, mean quantities and correlations are the same for all spins and pairs of spins, respectively. To automatically derive and solve the mean-field equations to second order, we make use of the QUANTUMCUMULANT.JL package [30], and present our code and the resulting equations in Secs. S2 and S3 of [14]. We obtain the average of the Dicke state quantum numbers from the first and second order mean values [20,22,23] as, $M = N(\langle\hat{\sigma}_1^{22}\rangle - \frac{1}{2})$ and $J = \sqrt{\frac{3}{4}N + N(N-1)(\langle\hat{\sigma}_1^{21}\hat{\sigma}_2^{12}\rangle + \langle\hat{\sigma}_1^{22}\hat{\sigma}_2^{22}\rangle - \langle\hat{\sigma}_1^{22}\rangle + \frac{1}{4})}$, where $\langle\hat{\sigma}_1^{22}\rangle$ is the population of the upper spin level and $\langle\hat{\sigma}_1^{21}\hat{\sigma}_2^{12}\rangle$, $\langle\hat{\sigma}_1^{22}\hat{\sigma}_2^{22}\rangle$ are correlations between different spins. The mean-field quantities and the Dicke state quantum numbers are different descriptions of the spin collective dynamics, but the latter provides more intuitive information on the spin-resonator collective coupling, cf. Figs. 2, 3, and 4.

Rabi oscillations and splitting at room temperature.—To observe collective Rabi oscillations, we drive the optically cooled spin ensemble with a resonant square microwave pulse of 1 μs duration, as in the experiment [7], and calculate the photon number inside the resonator, see Fig. 3(a). We observe that the photon number increases and decays with an oscillatory amplitude when the driving field switches on and off. Without the optical spin cooling $\eta_s = 0$ we observe no Rabi oscillations (black curve), while already for a weak cooling rate $\eta_s = 30$ Hz (blue dashed line), oscillations appear and become faster for higher rates $\eta_s = 10^2, 10^4$ Hz (red dash-dotted and green solid line), which confirms the increased coupling of the Dicke states with larger J [inset of Fig. 3(a)]. Note that the oscillations also end earlier for larger values of η_s. Rabi oscillations have been observed in room temperature experiments with pentacene molecules [12], but by a different mechanism,

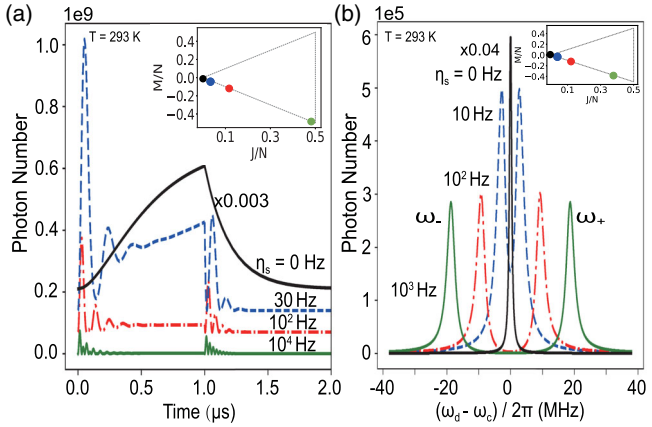

FIG. 3. Rabi oscillations and mode splitting at room temperature. Panel (a) shows the transient evolution of the photon number $\langle \hat{a}^\dagger \hat{a} \rangle$ inside the resonator subject to a short classical pulse for increasing spin-cooling rates $\eta_s = 0, 30, 10^2, 10^4$ Hz. The results are shifted vertically for clarity. Panel (b) shows the steady-state $\langle \hat{a}^\dagger \hat{a} \rangle$ as a function of detuning of the continuous microwave driving field around the resonator frequency for $\eta_s = 0, 10, 10^2, 10^3$ Hz. The inset panels show the Dicke states of the spin ensemble with increasing η_s. Here, we assume parameters compatible with the Rabi oscillation experiment at cryogenic temperature [7], e.g., the dephasing rate $2\pi \times 2.6$ MHz, see Sec. S4 of [14], and consider a dielectric resonator of same Q factor at room temperature (see Refs. [9–12]).

where thermally unoccupied triplet excited states were populated by optical pumping, and their subsequent collective coupling to a microwave resonator showed damped Rabi oscillations.

To observe the coherent splitting of the resonator transmission spectrum, we evaluate the steady-state photon number inside the resonator, as a function of the driving field frequency [Fig. 3(b)]. For no optical spin cooling $\eta_s = 0$, the resonator shows a conventional single peak, while a dip, known as the Fano effect in the weak coupling regime, appears already for a weak rate $\eta_s = 10$ Hz (blue dashed line). The dip evolves into two peaks, known as Rabi splitting in the strong coupling regime, for larger rates $\eta_s = 10^2, 10^3$ Hz (red dash-dotted and green solid line). This shows that by increasing η_s we make the spin ensemble occupy Dicke states with higher J values [inset of Fig. 3(b)], and thus explore CQED phenomena across the weak and strong coupling regimes.

Since the spin ensemble occupies states near the lower boundary of the Dicke state space, see the insets of Figs. 3(a) and 3(b), we may approximate these states as occupation number states of quantized harmonic oscillators (Holstein-Primakoff approximation [20,31,32]), and treat the spin-resonator system as two quantized harmonic oscillators coupled with strength $\sqrt{2J}g_s$. Furthermore, we can diagonalize the Hamiltonians for given J to yield two hybrid modes, see Sec. S5 of [14], which explains the two peaks split by $2\sqrt{2J}g_s$ under the resonant condition $\omega_s = \omega_c$ in Fig. 3(b). Since the value of J does not change much due to the driving of the resonator, we can determine the Rabi peak positions by our analytical expression for the mean value of J, as a function of the spin-lattice relaxation and optical spin-cooling rates. In Sec. S6 of [14], we show that by measuring the positions and heights of the Rabi peaks in the strong coupling regime, as in Fig. 3(b), we can sense the spin transition frequency. This permits sensing of related quantities, such as a magnetic field, in a regime different from the experiments [10,11], which applied the dispersive spin-resonator coupling in the weak coupling regime.

Stimulated superradiance pulses at room temperature.—We now study the transient excitation and subsequent collective decay of the spin ensemble at room temperature (Fig. 4). In our simulations, we drive the resonator with a strong microwave field to excite the spin ensemble ["(1)"], which is initially optically cooled to Dicke states with large J. Then, we switch off the microwave driving, and the spin ensemble dephases and decays toward lower excitation states with reduced J [inset of Fig. 4(b)], leading to the radiation pulse ["(2)"]. Finally, the optical spin-cooling and dephasing re-initialize the spin-ensemble into states with larger J ["(3)"]. The simulated photon number dynamics [Fig. 4(a)] is similar to the results observed in experiments at cryogenic temperature [8], but it occurs here with the optically cooled spin ensemble in an apparatus maintained

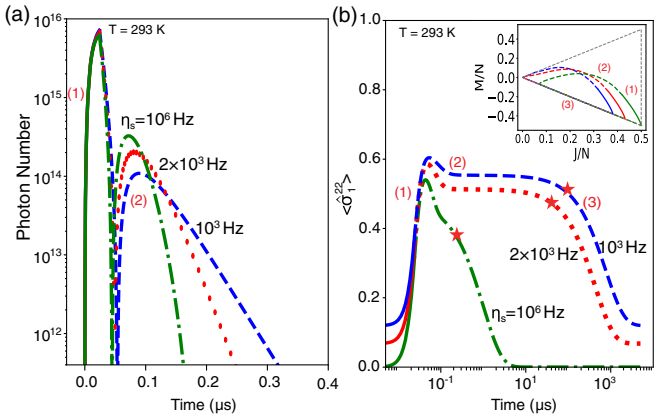

FIG. 4. Stimulated superradiance pulse of NV^- spins at room temperature. Panels (a) and (b) show the evolution of the intraresonator photon number (a), and the population of the upper spin state (b) (the inset shows the corresponding evolution of the Dicke state mean quantum numbers) during driving (1), stimulated superradiance (2), and spin recooling (3), for the optical spin-cooling rate $\eta_s = 10^3, 2 \times 10^3, 10^6$ Hz. The red stars mark the end of the superradiant phase. Here, we assume parameters compatible with the stimulated superradiance pulse experiment at cryogenic temperature [8], e.g., the dephasing rate $2\pi \times 4.7$ MHz, see Sec. S4 of [14], and consider a dielectric resonator of same Q factor at room temperature (see Refs. [9–12]).

at room temperature. We note that due to the strong spin dephasing, right after the emission the population of the upper spin state decays first to some finite value around 0.5, equivalent to Dicke states with small J [Fig. 4(b)]. Our results also show that the radiation pulses become stronger and shorter for larger values of η_s. Because of the involvement of the stimulated emission by the large number of photons and the exploration of collective Dicke states, the radiation is qualified as stimulated superradiance.

Conclusions.—In summary, we have demonstrated theoretically that optical pumping can counteract thermalization of spin states in a room temperature environment, and prepare and maintain a NV^- spin-ensemble in Dicke states with high symmetry and strong collective coupling to a microwave resonator. Using parameters compatible with existing experimental setups, we show that CQED effects, such as Rabi oscillations, Rabi splitting, and stimulated superradiance, can be realized at room temperature. The mechanisms as revealed may enable further applications and studies of quantum dynamics such as quantum memories [33] and self-stimulated spin echoes [34] in ambient environments.

In our calculations, we modeled the spins as two-level systems to represent the main physical properties and to reach qualitative conclusions for the spin system. More elaborate and advanced theory is required to describe quantitatively the influence of subtle details, such as the multilevel structure and the resulting presence of different transitions, on the optical spin cooling [21]. Such analysis could also address the possible transitions between the upper spin levels [35] and the effects of the optical heating of the diamond. However, our preliminary attempts in this direction indicate no qualitative differences from the conclusions achieved here [27]. We note that, after the reprint of our work was reported and during its review for publication, an experimental work appeared as a reprint [36], and reported independently the observation of laser power-controlled Rabi splittings, confirming our theoretical prediction.

We acknowledge Hao Wu for helpful discussions on the physics and the manuscript. This work was supported by the National Natural Science Foundation of China through the Projects No. 12004344 and No. 62027816, and Henan Center for Outstanding Overseas Scientists Project No. GZS201903, as well as the Danish National Research Foundation through the Center of Excellence for Complex Quantum Systems (Grant agreement No. DNRF156). Y. Z. and Q. W. contributed equally to this work. All the authors contributed to the writing of the manuscript.

*yzhuaudipc@zzu.edu.cn
†cxshan@zzu.edu.cn
‡moelmer@phys.au.dk

[1] H. Mabuchi and A. C. Doherty, Cavity quantum electrodynamics: Coherence in context, Science **298**, 1372 (2002).
[2] J. M. Raimond, M. Brune, and S. Haroche, Manipulating quantum entanglement with atoms and photons in a cavity, Rev. Mod. Phys. **73**, 565 (2001).
[3] J. Ye, H. J. Kimble, and H. Katori, Quantum state engineering and precision metrology using state-insensitive light traps, Science **320**, 1734 (2008).
[4] R. Amsüss, Ch. Koller, T. Nöbauer, S. Putz, S. Rotter, K. Sandner, S. Schneider, M. Schramböck, G. Steinhauser, H. Ritsch, J. Schmiedmayer, and J. Majer, Cavity QED with Magnetically Coupled Collective Spin States, Phys. Rev. Lett. **107**, 060502 (2011).
[5] Y. Kubo, F. R. Ong, P. Bertet, D. Vion, V. Jacques, D. Zheng, A. Dréau, J.-F. Roch, A. Auffeves, F. Jelezko, J. Wrachtrup, M. F. Barthe, P. Bergonzo, and D. Esteve, Strong Coupling of a Spin Ensemble to a Superconducting Resonator, Phys. Rev. Lett. **105**, 140502 (2010).
[6] A. Angerer, T. Astner, D. Wirtitsch, H. Sumiya, S. Onoda, J. Isoya, S. Putz, and J. Majer, Collective strong coupling with homogeneous Rabi frequencies using a 3D lumped element microwave resonator, Appl. Phys. Lett. **109**, 033508 (2016).
[7] S. Putz, D. O. Krimer, R. Amsüss, A. Valookaran, T. Nöbauer, J. Schmiedmayer, S. Rotter, and J. Majer, Protecting a spin ensemble against decoherence in the strong-coupling regime of cavity QED, Nat. Phys. **10**, 720 (2014).
[8] A. Angerer, K. Streltsov, T. Astner, S. Putz, H. Sumiya, S. Onoda, J. Isoya, W. J. Munro, K. Nemoto, J. Schmiedmayer, and J. Majer, Superradiant emission from colour centres in diamond, Nat. Phys. **14**, 1168 (2018).
[9] J. D. Breeze, E. Salvadori, J. Sathian, N. M. Alford, and C. W. M. Kay, Continuous-wave room-temperature diamond maser, Nature (London) **555**, 493 (2018).
[10] E. R. Eisenach, J. F. Barry, M. F. O'Keeffe, J. M. Schloss, M. H. Steinecker, D. R. Englund, and D. A. Braje, Cavity-enhanced microwave readout of a solid-state spin sensor, Nat. Commun. **12**, 1357 (2021).
[11] J. Ebel, T. Joas, M. Schalk, P. Weinbrenner, A. Angerer, J. Majer, and F. Reinhard, Dispersive readout of room temperature spin sensors, Quantum Sci. Technol. **6**, 03LT01 (2021).
[12] J. D. Breeze, E. Salvadori, J. Sathian, N. M. Alford, and C. W. M. Kay, Room-temperature cavity quantum electrodynamics with strongly coupled Dicke states, npj Quantum Inf. **3**, 40 (2017).
[13] R. H. Dicke, Coherence in spontaneous radiation processes, Phys. Rev. **93**, 99 (1954).
[14] See Supplemental Material at http://link.aps.org/supplemental/10.1103/PhysRevLett.128.253601 for extra theoretical derivations, numerical simulations and discussions, which includes Ref. [15].
[15] A. Norambuena, E. Muñoz, H. T. Dinani, A. Jarmola, P. Maletinsky, D. Budker, and J. R. Maze, Spin-lattice relaxation of individual solid-state spins, Phys. Rev. B **97**, 094304 (2018).
[16] Y. Zhang, Y-X. Zhang, and K. Mølmer, Monte-Carlo simulations of superradiant lasing, New J. Phys. **20**, 112001 (2018).
[17] B. Q. Baragiola, B. A. Chase, and J. M. Geremia, Collective uncertainty in partially polarized and partially decohered spin-$\frac{1}{2}$ systems, Phys. Rev. A **81**, 032104 (2010).

[18] N. Shammah, S. Ahmed, N. Lambert, S. De Liberato, and F. Nori, Open quantum systems with local and collective incoherent processes: Efficient numerical simulations using permutational invariance, Phys. Rev. A **98**, 063815 (2018).
[19] J. Wesenberg and K. Mølmer, Mixed collective states of many spins, Phys. Rev. A **65**, 062304 (2002).
[20] Q. Wu, Y. Zhang, X. Yang, S.-L. Su, C. X. Shan, and K. Mølmer, A superradiant maser with nitrogen-vacancy center spins, Sci. China-Phys. Mech. Astron. **65**, 217311 (2022).
[21] W. Ng, H. Wu, and M. Oxborrow, Quasi-continuous cooling of a microwave mode on a benchtop using hyperpolarized NV^- diamond, Appl. Phys. Lett. **119**, 234001 (2021).
[22] K. Debnath, Y. Zhang, and K. Mølmer, Lasing in the superradiant crossover regime, Phys. Rev. A **98**, 063837 (2018).
[23] Y. Zhang, C. X. Shan, and K. Mølmer, Ultranarrow Superradiant Lasing by Dark Atom-photon Dressed States, Phys. Rev. Lett. **126**, 123602 (2021).
[24] C. J. Wood and D. G. Cory, Cavity cooling to the ground state of an ensemble quantum system, Phys. Rev. A **93**, 023414 (2016).
[25] T. Astner, J. Gugler, A. Angerer, S. Wald, S. Putz, N. J. Mauser, M. Trupke, H. Sumiya, S. Onoda, J. Isoya, J. Schmiedmayer, P. Mohn, and J. Majer, Solid-state electron spin lifetime limited by phononic vacuum modes, Nat. Mater. **17**, 313 (2018).
[26] A. Jarmola, V. M. Acosta, K. Jensen, S. Chemerisov, and D. Budker, Temperature- and Magnetic-Field-Dependent Longitudinal Spin Relaxation in Nitrogen-Vacancy Ensembles in Diamond, Phys. Rev. Lett. **108**, 197601 (2012).
[27] Y. Zhang, Q. Wu, H. Wu, X. Yang, S.-L. Su, C. X. Shan, and K. Mølmer, Cavity quantum electrodynamics effects of optically cooled nitrogen-vacancy centers coupled to a high frequency microwave resonator, arXiv:2203.04102.
[28] A. Bychek, C. Hotter, D. Plankensteiner, and H. Ritsch, Superradiant lasing in inhomogeneously broadened ensembles with spatially varying coupling, Open Res. Eur. **1**, 73 (2021).
[29] H. A. M. Leymann, A. Foerster, and J. Wiersig, Expectation value based equation-of-motion approach for open quantum systems: A general formalism, Phys. Rev. B **89**, 085308 (2014).
[30] D. Plankensteiner, C. Hotter, and H. Ritsch, QuantumCumulants.jl: A Julia framework for generalized mean-field equations in open quantum systems, Quantum **6**, 617 (2022).
[31] J. A. Gyamfi, An introduction to the Holstein-Primakoff transformation, with applications in magnetic resonance, arXiv:1907.07122.
[32] T. Holstein and H. Primakoff, Field dependence of the intrinsic domain magnetization of a ferromagnet, Phys. Rev. **58**, 1098 (1940).
[33] I. Diniz, S. Portolan, R. Ferreira, J. M. Gérard, P. Bertet, and A. Auffèves, Strongly coupling a cavity to inhomogeneous ensembles of emitters: Potential for long-lived solid-state quantum memories, Phys. Rev. A **84**, 063810 (2011).
[34] K. Debnath, G. Dold, J. J. L. Morton, and K. Mølmer, Self-Stimulated Pulse Echo Trains from Inhomogeneously Broadened Spin Ensembles, Phys. Rev. Lett. **125**, 137702 (2020).
[35] M. C. Cambria, A. Gardill, Y. Li, A. Norambuena, J. R. Maze, and S. Kolkowitz, State-dependent phonon-limited spin relaxation of nitrogen-vacancy centers. Phys. Rev. Research **3**, 013123 (2021).
[36] D. P. Fahey, K. Jacobs, M. J. Turner, H. Choi, J. E. Hoffman, D. Englund, and M. E. Trusheim, Steady-state microwave mode cooling with a diamond NV ensemble, arXiv:2203.03462.